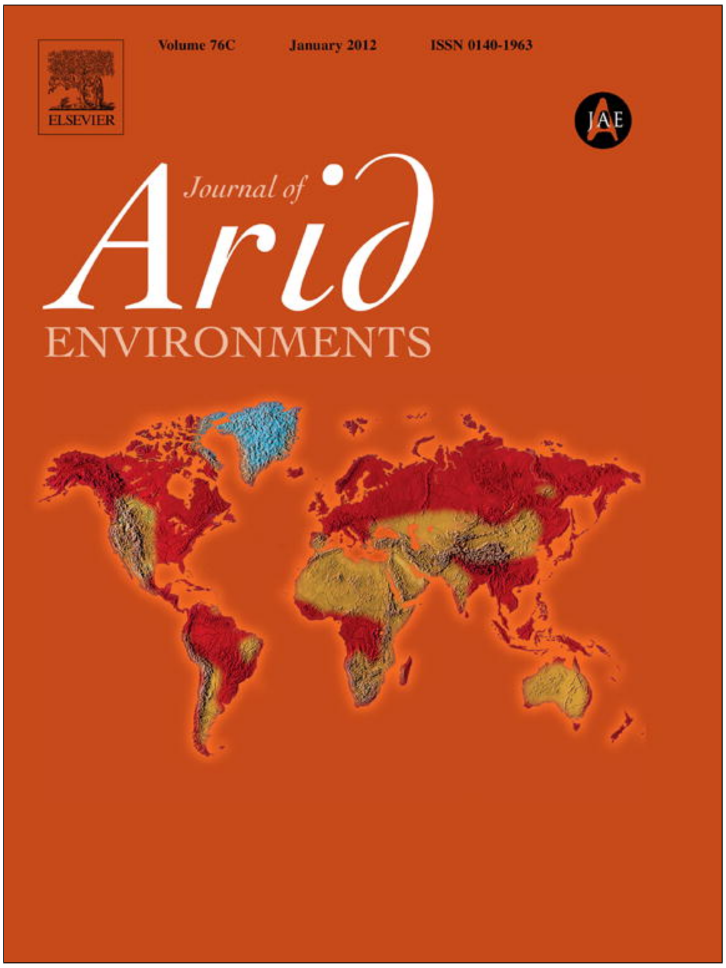

(This is a sample cover image for this issue. The actual cover is not yet available at this time.)

Journal of Arid Environments 82 (2012) 11–18

Contents lists available at SciVerse ScienceDirect

Journal of Arid Environments

journal homepage: www.elsevier.com/locate/jaridenv

The use of precipitation intensity in estimating gross primary production in four northern grasslands

C. Wu [a,b,*], J.M. Chen [a]

[a] Department of Geography, University of Toronto, 100 St. George St., Room 5047, Toronto, ON M5S 3G3, Canada
[b] The State Key Laboratory of Remote Sensing Science, Institute of Remote Sensing Applications, Chinese Academy of Sciences, Beijing 100101, China

ARTICLE INFO

Article history:
Received 10 June 2011
Received in revised form
9 December 2011
Accepted 19 February 2012
Available online xxx

Keywords:
Climate change
Grasslands
Gross primary production
MODIS
Precipitation intensity

ABSTRACT

Remote sensing is a useful tool for the estimation of gross primary production (GPP) in terrestrial ecosystems at regional to global scales. One limitation of remote sensing based GPP models is the inappropriate characterizing of precipitation impacts. In this study, we showed positive relationship between the monthly flux-measured GPP of four grasslands ecosystems and the precipitation intensity, which was calculated from dividing the monthly sums of precipitation by the half-hourly precipitation frequency. Suggested by this finding, two remote sensing based GPP models, i.e. the greenness and radiation model (GR) and the temperature and greenness (TG) model, were selected to test the potential of incorporating this precipitation intensity for the estimation of monthly GPP. A scaled precipitation intensity was proposed by normalizing a multi-year maximum precipitation intensity, considering its dynamical ranges across sites and regions. Results indicated that by adding of this scalar, the revised models can provide better monthly GPP estimates with average 10% improvements in precisions compared to their original outputs. A further analysis showed that such better performances of the revised models can be attributed to the positive relationship between precipitation intensity and the absorbed photosynthetically active radiation (APAR). However, no evident response has been observed on the light use efficiency (LUE), indicating the LUE and precipitation intensity relationship may differ across species and ecoregions. To the best of our knowledge, this is the first report of the potential use of precipitation intensity in the remote sensing based GPP models and it will be useful for the development of future models that can better predict GPP in the context of future precipitation regimes.

1. Introduction

Terrestrial ecosystems play a dynamic role in the global carbon (C) cycle as the carbon balance of terrestrial ecosystems is highly sensitive to climate changes, such as the inter-annual variations of precipitation regimes and increased surface temperatures as a result of the increase in atmospheric greenhouse gases (Beer et al., 2010). The increase in temperature and the elevated CO_2 in the atmosphere have been demonstrated to have great effects on terrestrial ecosystem production (Norby et al., 2005; Zhao and Running, 2010). Precipitation, on the contrary, has been suggested to have a more profound impact on ecosystem dynamics, especially in arid and semiarid environments (Weltzin et al., 2003). Changes in global and regional precipitation regimes are expected to have ramifications for the distribution, structure, and diversity of plants (Easterling et al., 2000). Although there are uncertainties for the feedbacks between annual precipitation variability and the aboveground net primary production (ANPP), it is suggested that precipitation patterns can alter the vegetation production and the responses may differ across biomes (Fang et al., 2001; Knapp and Smith, 2001).

Remote sensing has been an important tool for the estimation of gross primary production (GPP) at large spatial scales. Most of these models are based on the capturing of spectral characteristics of vegetation that are correlated to the biomass production. Specifically, the vegetation index (VI) are widely used in such models, providing an indicator of either the light use efficiency (LUE) (Garbulsky et al., 2011) or the faction of the absorbed photosynthetically active radiation (f_{APAR}) (Xiao et al., 2004). For example, the temperature and greenness (TG) model, derived by Sims et al. (2008), utilizes a combination of the enhanced vegetation index (EVI, Huete et al., 2002) and the land surface temperature (LST) in estimating GPP across different biomes. A total chlorophyll based model using the product of the normalized difference vegetation index (NDVI, Rouse et al., 1974) and incoming photosynthetically active radiation (PAR) also shows promising results for estimating

* Corresponding author. Tel.: +1 647 524 0310.
E-mail address: hefery@163.com (C. Wu).

0140-1963/$ – see front matter © 2012 Elsevier Ltd. All rights reserved.
doi:10.1016/j.jaridenv.2012.02.014

GPP in crops (Gitelson et al., 2006; Wu et al., 2009) and forest landscapes (Wu et al., 2010). A common limitation of these remote sensing based GPP models is the inappropriate characterizing of the meteorological factors (e.g., temperature, precipitation) that can greatly affect LUE, leading to the largest uncertainty constrains the application of these models globally (Mu et al., 2011; Zhao et al., 2006). The reason is that the real-time LUE would change dramatically across seasons and between vegetation types that would be a function of factors as chlorophyll content, light, water, temperature (Hilker et al., 2008; Sims et al., 2008; Zhao et al., 2006) and thus a single vegetation index may have limited ability in LUE estimation, especially in extreme drought conditions (Samanta et al., 2010).

While impact on changes in the surface temperature has been considered in many GPP models (e.g., Coops et al., 2005; Sims et al., 2008; Xiao et al., 2004), little attention and result have been reported on views of precipitation regimes in such remote sensing based GPP models. Furthermore, precipitation regimes are predicted to become more variable with more extreme rainfall events punctuated by longer intervening dry periods. Manipulated experiments have demonstrated that these changes in patterns of precipitation can alter vegetation production (Heisler-White et al., 2008; Thomey et al., 2011). Therefore, it is urgent and necessary to improve those GPP models with incorporation of precipitation regimes, especially in consideration of the future regional and global climate changes (Paiva et al., 2011). Here we reported an analysis of the potential use of the precipitation intensity in remote sensing based GPP models. Satellite observations from the Moderate Resolution Imaging Spectroradiometer (MODIS) images and multi-year flux measurements were used to estimate monthly GPP in four northern grasslands. The objectives are (1) to explore the potential for GPP estimation by incorporation of precipitation intensity, (2) to give analyses of reasons for the better performance of the revised models. These results will be useful for the development of future GPP models based on remote sensing observations and climate variables.

2. Materials and method

2.1. Study sites

To support the analysis of this study, four grasslands were selected in North America (Fig. 1). The first site is located west of Lethbridge, Alberta, Canada, referred as CA-LET hereafter. This site is classified as mixed grassland and occurs in the northern portion of the Great Plains, which is the second largest eco-zone in North America, covering approximately 2.6 million square kilometers. The plant community is consisted of the dominant grasses of *Agropyron dasystachyum* [(Hook.) Scrib.] and *Agropyron smithii* (Rydb.) (Flanagan and Johnson, 2005). The second site is located in an open grassland ecosystem in the foothills of the Sierra Nevada in California, USA, referred as US-VAR hereafter. This site is classified as grassland dominated by C3 annual grasses, mainly including Purple false brome (*Brachypodium distachyon* L.) and Smooth cat's ear (*Hypochaeris glabra* L.). The third grassland site is located in the Audubon Research Ranch, Sonoita Valley, Arizona, USA, which is the largest ungrazed, privately managed grassland sites in Arizona (Krishnan et al., 2011). Dominant species include the short-grass prairie (C4 perennial bunchgrasses, primarily *Bouteloua gracilis*, *Bouteloua curtipendula*, and *Eragrostis intermedia*) and two lovegrasses (Lehmann lovegrass (*Eragrostis lehmanniana*) and Boer lovegrass (*Eragrostis curvula* var. *conferta*)). The final site is the walnut river watershed site (US-WLR), which rests on a C3/C4 mixed grassland, tallgrass prairie north of Manhattan, Kansas, USA. The dominate species are two C4 grasses (*Andropogon gerardii* Vitman and *Sorghastrum nutans* [L.] Nash). Subdominants include the C3 grass *Poa pratensis* L. and the C4 grasses *B. curtipendula* (Michx.) Torr (Jastrow et al., 2000). Detailed descriptions for each site and the relative references were shown in Table 1.

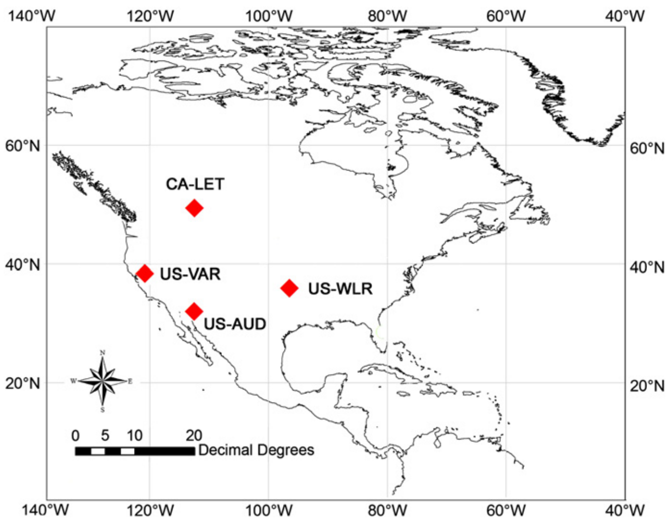

Fig. 1. Spatial distribution of the four grassland sites in this study.

2.2. Flux measurements and climate data

Flux data of site CA-LET were downloaded from the Fluxnet Canada Data Information System (http://www.fluxnet-canada.ca) while data for the remaining three US sites were acquired from http://public.ornl.gov/ameriflux/dataproducts.shtml.

Meteorological variables of air temperature (T_a, °C), precipitation and radiation were measured from site sensors. Precipitation data of these sites were obtained from the gap-filled half-hourly meteorological measurements collected by on-site tipping bucket sensors. Besides of sums of monthly precipitation quantity, we also calculated the half-hourly precipitation frequency (n), which was determined as the number of time periods with observed precipitation. The precipitation intensity (P_a, mm/0.5 h) was then obtained from dividing the sums of monthly precipitation by the precipitation frequency (n) from the half-hourly observations.

The monthly GPP was also acquired for each site. For CA-LET, a standard procedure by the Fluxnet-Canada Research Network was used to estimate monthly net ecosystem production (NEP) and to partition NEP into components of GPP and ecosystem respiration (Re) (Barr et al., 2004). The procedure to estimate monthly GPP from half-hour measurements of NEP first derives GPP and Re from measured NEP and then fills gaps in GPP, Re and NEP using simple empirical models that are constrained by the measured data. For the other three US sites, the level-4 monthly GPP product was used and these data were gap-filled with the Artificial Neural Network (ANN) method (Papale and Valentini, 2003) and/or the Marginal Distribution Sampling (MDS) method (Reichstein et al., 2005).

2.3. MODIS products

To support the satellite estimation of GPP, two MODIS products were used which were acquired at https://lpdaac.usgs.gov/lpdaac/get_data/wist.

The first MODIS product is the Terra MODIS 8-day LAI product (MOD15 A2, 1 km), which provides LAI data globally (Yang et al., 2006). The second product is the 8-day Terra MODIS surface reflectance atmospheric correction algorithm product (MOD09A1,

Table 1
Description of the four grasslands sites in this study.

Site ID	Site name	Latitude	Longitude	Precipitation (mm/yr)	Climate	Time range	References
CA-LET	Lethbridge	49.43 N	−112.56 E	398	Temperate continental	2002–2005	Flanagan et al., 2002
US-VAR	Vaira Ranch	38.41 N	−120.95 E	544	SubTropical-Mediterranean	2003–2006	Ryu et al., 2008
US-AUD	Audubon Research Ranch	31.59 N	−110.51 E	438	Temperate arid	2003–2005	Krishnan et al., 2011
US-WLR	WalnutRiver	37.52 N	−96.85 E	995	Temperate continental	2002–2004	Jastrow et al., 2000

500 m) which provides surface reflectance data at seven bands from optical to shortwave ranges. These reflectance were used to derive two vegetation indices, including the NDVI and EVI with the equations below,

$$\mathrm{NDVI} = (R_{\mathrm{NIR}} - R_{\mathrm{red}})/(R_{\mathrm{NIR}} + R_{\mathrm{red}}) \tag{1}$$

$$\mathrm{EVI} = 2.5 \times \frac{R_{\mathrm{NIR}} - R_{\mathrm{Red}}}{1 + R_{\mathrm{NIR}} + 6 \times R_{\mathrm{Red}} - 7.5 \times R_{\mathrm{Blue}}} \tag{2}$$

where the R_x represents the reflectance at the given wavelength (nm).

We only used the MODIS LAI data for US-AUD and US-WLR where in situ data was unavailable. For these two sites, the LAI data of the central pixel was extracted to represent the value of flux towers considering the footprints at each directions were around 1.5 km for both sites. Both NDVI and EVI were used for all sites and were extracted from 3 × 3 MODIS pixels centered on the flux tower similar to the approach used by Sims et al. (2008) and Wu et al. (2011). The 3 × 3 MODIS pixels method was also checked at each site with respect to footprints at each direction. Both 8-day LAI and vegetation indices observed during the month were then averaged to represent the mean monthly value.

2.4. Ground LAI and LUE calculations

For CA-LET and US-VAR, ground measured LAI were available and thus were used. LAI was measured once every two weeks by destructive sampling (0.2 m × 0.5 m, replicates = 6) using a leaf area meter (model LI-3100, LI-COR Inc.) in CA-LET. All observations within the same month were averaged to represent the mean monthly value. Detail descriptions of LAI sampling are shown in Flanagan et al. (2002). For US-VAR, the LAI was determined by harvesting four sample plots (0.25 m × 0.25 m) within the footprint of flux tower based on the extrapolation of data obtained during periodic field visits (Ryu et al., 2008).

These LAI data were further used to determine the faction of APAR (f_{APAR}) by the following equation and with the light extinction coefficient ($k = 0.5$),

$$f_{\mathrm{APAR}} = 0.95 \times \left(1 - e^{-k\mathrm{LAI}}\right) \tag{3}$$

For the other two sites (US-AUD and US-WLR) where in situ LAI were unavailable, the f_{APAR} of these two sites were calculated from an alternative method, considering the widely reported relationship between the f_{APAR} and the NDVI,

$$f_{\mathrm{APAR}} = 1.24 \times \mathrm{NDVI} - 0.168 \tag{4}$$

The empirical relationship between f_{APAR} and NDVI we used has been validated in diverse ecosystems in North America (Wu et al., 2011), which gives us more confidence in use this correlation.

The monthly LUE of all sites then can be determined by the flux-measured GPP, f_{APAR} and PAR from meteorological measurements using equation below:

$$\mathrm{LUE} = \frac{\mathrm{GPP}}{f_{\mathrm{APAR}} \times \mathrm{PAR}} \tag{5}$$

Growing seasons for these sites were different considering their local climates. Owing to a Mediterranean climate for site US-VAR, months from May to Oct. were excluded because GPP in these non-growing season months were zero (Ryu et al., 2008). For the other three sites, months from May to Oct. were selected (Flanagan et al., 2002; Jastrow et al., 2000; Krishnan et al., 2011).

2.5. Description of GPP models

Two remote sensing based GPP models were selected. The first is the greenness and radiation model (GR) which is firstly proposed by Gitelson et al. (2006) in both irrigated and rainfed maize. Later validations of the model also show promising results in different crops (Wu et al., 2009) as well as forest landscapes (Wu et al., 2011). The underlying mechanism of this model lies in the correlation between the GPP and the total canopy chlorophyll content. Therefore, vegetation indices that derived to be proxies of total chlorophyll content can be used in the estimation of GPP with combination of the incoming PAR. Briefly, the model can be expressed by the following equation,

$$\mathrm{GPP} = \mathrm{EVI} \times \mathrm{PAR} \tag{6}$$

A second model is the temperature and greenness (TG) model proposed by Sims et al. (2008) that estimates GPP using a combination of MODIS LST and EVI products. The most important merit of this model is the independence of climate variables. The original form of the TG model can be illustrated by,

$$\mathrm{GPP} = \mathrm{ScaledEVI} \times \mathrm{ScaledLST} \tag{7}$$

Empirical data suggests that GPP may drop to zero when EVI is around 0.1 and thus the ScaledEVI is determined as:

$$\mathrm{ScaledEVI} = \mathrm{EVI} - 0.1 \tag{8}$$

The ScaledLST is proposed based on the determination of optimum temperature for GPP. As GPP generally increases to the maximum values at the LST around 30 °C, two linear equations are used to define the ScaledLST,

$$\mathrm{ScaledLST} = \min[(\mathrm{LST}/30), (2.5 - 0.05 \times \mathrm{LST})] \tag{9}$$

However, the use of MODIS LST can lead uncertainties because satellite sensors measure a signal that is a combination of the radiant temperature of the land surface and the intervening atmosphere (Goetz et al., 2000). Therefore, we used a simple revised form of the original model with the T_a from the flux measurements considering all monthly temperature in our analysis were below 30 °C,

$$\mathrm{GPP} = \mathrm{EVI} \times T_a \tag{10}$$

2.6. Statistical analyses

In order to analyze different drivers on monthly GPP, both meteorological variables (i.e., temperature and precipitation) and canopy parameters (i.e., LAI and EVI) were tested and compared.

Considering the dynamical ranges of these variables across sites and regions, we explored the correlations between GPP and these variables by exploration of their month-to-month anomalies, allowing the identification and evaluation of these correlations within sites and excluding errors from spatial interference. The pairwise Pearson coefficient (r) and p-value were used to assess these correlations. When considering the GPP model performances, observations across all sites were used to test and show the robustness of models. The coefficient of determination (R^2) and the p-value were accordingly used to evaluate the relationship.

3. Results

3.1. Meteorological and canopy factors on monthly GPP

We first analyzed the meteorological factors i.e., temperature and precipitation, on monthly GPP across all sites using the month-to-month anomalies (Fig. 2). Monthly temperature showed a positive impacts on GPP with a Pearson coefficient r of 0.46 ($p < 0.001$) for the overall dataset. This trend also existed for data of each individual site with slight differences in degrees. The monthly precipitation quantity, however, was not found to be correlated with monthly GPP as no significant correlation was observed for the overall dataset ($r = 0.08$, $p = 0.494$). We also explored this correlation for each single site and none of these correlations were significant. The Pearson coefficient r for CA-LET, US-VAR, US-AUD and US-WLR were 0.02 ($p = 0.919$), 0.34 ($p = 0.137$), 0.38 ($p = 0.158$) and 0.29 ($p = 0.313$), respectively. These observations suggest that the monthly precipitation is not a reliable indicator of GPP. On the contrary, when the precipitation intensity was correlated with GPP, we identified a significant relationship for the overall dataset with r of 0.39 ($p = 0.001$). Data for individual site also indicates that the P_a is a better proxy than the precipitation quantity of monthly GPP. While P_a was not significantly correlation with monthly GPP for US-AUD ($r = 0.11$, $p = 0.568$), we acquired significant relationships for all the other three sites with r of 0.73 ($p < 0.001$), 0.52 ($p = 0.018$) and 0.46 ($p = 0.042$) for CA-LET, US-VAR and US-WLR, respectively.

Two canopy variables, including the LAI and EVI, were selected to test their impacts on monthly GPP (Fig. 3). LAI was demonstrated as a good indicator of monthly GPP with a Pearson coefficient r of 0.62 ($p < 0.001$) for all observations, suggesting a positive influence of LAI on GPP. This strong correlation also existed for each individual site with r ranging from 0.45 ($p = 0.042$) for US-VAR to 0.93 ($p < 0.001$) for US-WLR. Canopy EVI showed high correlation with monthly GPP and an r of 0.71 ($p < 0.001$) was acquired for the overall dataset, implying the potential of EVI as an indicator of GPP.

3.2. GPP estimation with incorporation of precipitation intensity

We first estimated the monthly GPP using the two original models (Fig. 4). Both the GR model and the TG model can provide reasonable estimates of monthly GPP with coefficients of determination (R^2) of 0.71 ($p < 0.001$) and 0.58 ($p < 0.001$), and root mean square errors (RMSE) of 46.1 g C m^{-2} month^{-1} and 55.3 g C m^{-2} month^{-1}, respectively. The GR model was first produced for GPP estimation in crops, and results in our testing indicate that this model may have the potential for the application of GPP estimation in grasslands, probably due to similar canopy structures between these two ecosystems. Furthermore, the GR model generally showed a better performance than the TG model, both for most of the individual sites and the overall dataset (Table 2). These results agree with recently evaluation of both models at various ecosystems in North America (Wu et al., 2011).

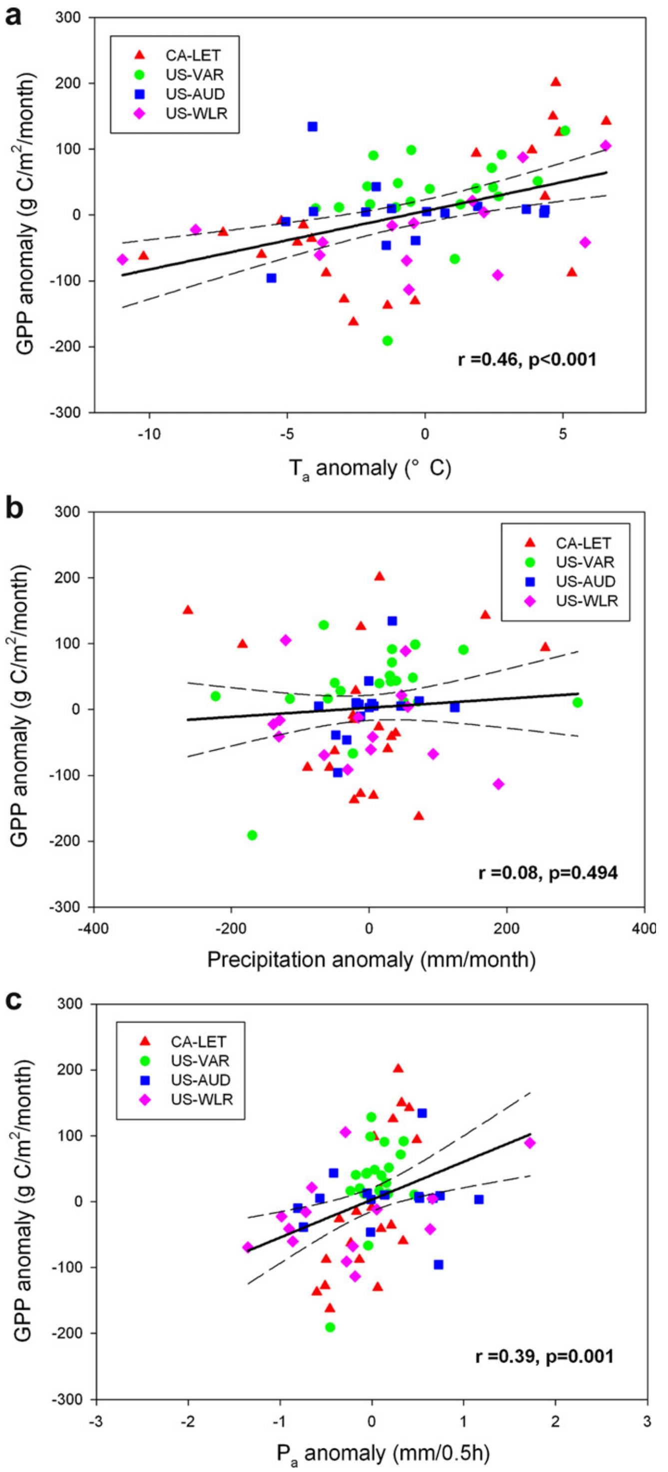

Fig. 2. Relationships between monthly anomalies of GPP and (a) air temperature (T_a), (b) precipitation and (c) precipitation intensity (P_a).

In view as a meteorological scalar, we first multiplied the original algorithms by P_a for the two models (i.e., $P_a \times$ GR and $P_a \times$ TG), expecting to show the influence of precipitation intensity on GPP estimation. As expected, this simple multiplication produced improved GPP estimates at individual sites with both models (Table 3). One exception was the US-WLR where a slightly lower correlation was observed for the revised model ($R^2 = 0.79$, $p < 0.001$) compared with the original GR ($R^2 = 0.81$, $p < 0.001$).

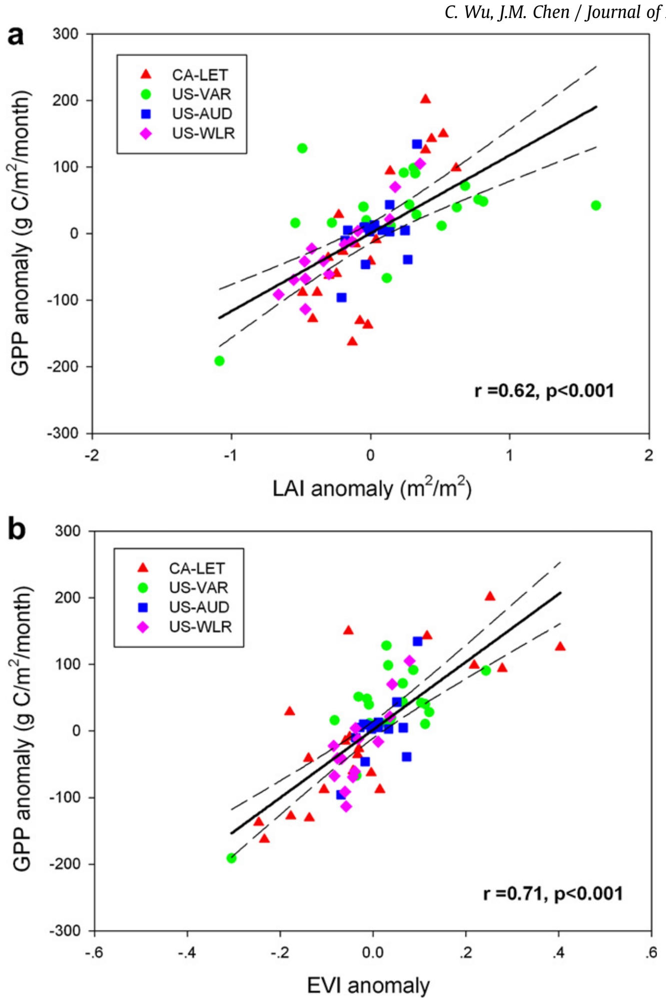

Fig. 3. Relationships between monthly anomalies of GPP and (a) leaf area index (LAI) and (b) enhanced vegetation index (EVI).

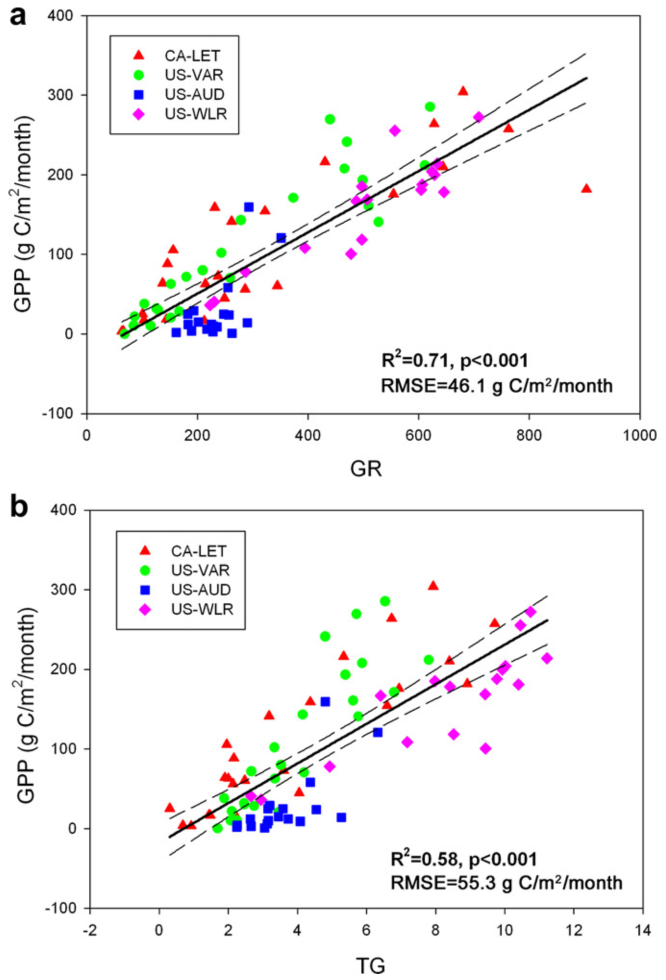

Fig. 4. Estimating monthly GPP using the (a) greenness and radiation (GR) model and (b) the temperature and greenness (TG) model.

However, the largest limitation of this simple revision was the inappropriate performances for the overall dataset, which indicates that this method is not workable across sites and regions (Fig. 5). For mesic grassland site US-WLR, the average P_a was about 2.23 mm/0.5 h, which is substantially larger than the other three sites (0.85 mm/0.5 h). This site difference leads to a different dynamical range of the mesic site and thus the low precision of GPP estimates for the overall dataset.

To correct this regional climate difference, we proposed a modified P_a scalar as:

$$\mathrm{Scaled}P_a = P_{ai}/P_{amax} \tag{11}$$

where P_{ai} is the precipitation intensity in month i, and P_{amax} represents the maximum P_a for this site from multi-year observations. We suspect that incorporating a multi-year maximum P_a may be potentially helpful for capturing the effects of both seasonal and inter-annual variations of precipitation regimes. Furthermore, by normalizing with P_{amax}, site difference with respect to the range of precipitation intensity can be reduced.

Using this ScaledP_a, we observed evident effect in correcting the site specific climate difference and the results were much improved for data of both individual site and the overall dataset compared to the original GR and TG models (Fig. 6 and Table 4). The revised models (i.e. Scaled$P_a \times$ GR and Scaled$P_a \times$ TG) gave RMSE of 40.8 g C m^{-2} month^{-1} and 50.2 g C m^{-2} month^{-1}, respectively, which was about 10% improvement in the precision. At each site, the revised model also produced better GPP estimates, implying the high potential use of the precipitation intensity in future GPP models.

4. Discussion

4.1. Relationship between P_a and GPP

Annual precipitation increase is demonstrated to have positive effects on annual GPP (Beer et al., 2010), however, at monthly temporal scale, influences of changes in precipitation patterns are

Table 2
Comparison between original model performances for each site.

Sites		GPP models	
		GR	TG
CA-LET	R^2	0.71	0.79
	RMSE	48.1	41.2
US-VAR	R^2	0.85	0.77
	RMSE	59.2	61.9
US-AUD	R^2	0.48	0.46
	RMSE	32.7	32.0
US-WLR	R^2	0.81	0.72
	RMSE	29.2	34.8

Note: RMSE in GPP unit of g C m^{-2} month^{-1}.

Table 3
Comparison between model performances for each site.

Sites		GPP models	
		$P_a \times$ GR	$P_a \times$ TG
CA-LET	R^2	0.85	0.86
	RMSE	34.4	33.1
US-VAR	R^2	0.87	0.81
	RMSE	31.5	44.0
US-AUD	R^2	0.49	0.53
	RMSE	29.6	28.7
US-WLR	R^2	0.79	0.77
	RMSE	31.7	31.9

Note: RMSE in GPP unit of g C m^{-2} $month^{-1}$.

not well known. Our results conducted at four grasslands show that the precipitation quantity is not a good indicator of GPP at monthly temporal scale. On the contrary, the precipitation intensity is a better indictor than the precipitation quantity of variability, and thus shows a potential use for tracking variations in GPP (Heisler-White et al., 2008). This positive correlation between P_a and GPP can be supported by the previous work of altered rain size in grassland (Knapp et al., 2008) and it also coincides with a recent research of Thomey et al. (2011), which reports a significant increase of above net primary production for grassland with an extra single large rainfall event than samples receiving multiple small events with equal total rainfall amounts.

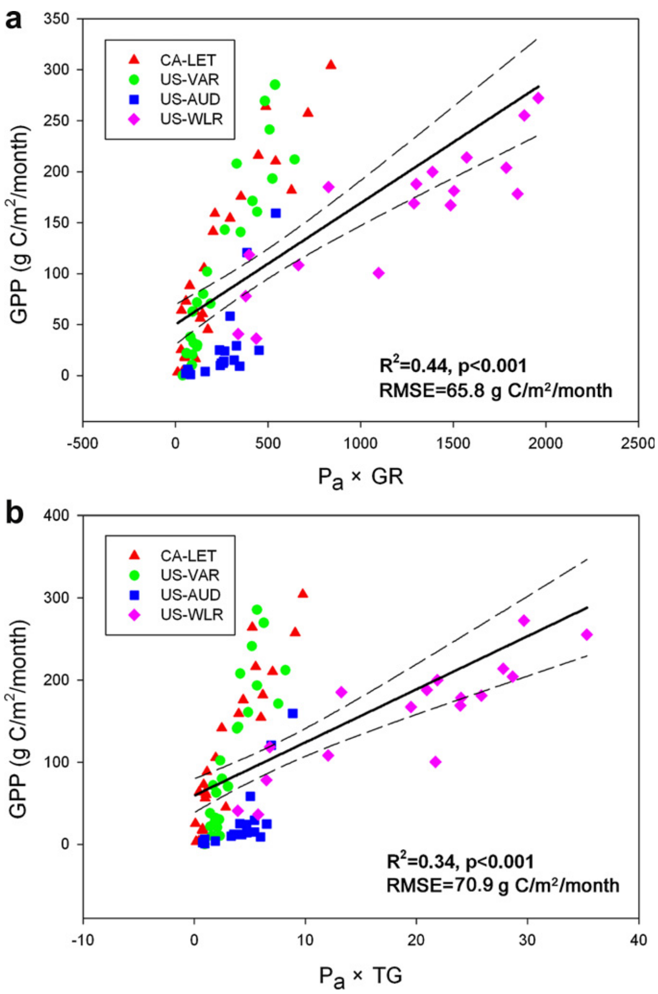

Fig. 5. Estimating monthly GPP using the (a) $P_a \times$ GR model and (b) $P_a \times$ TG model.

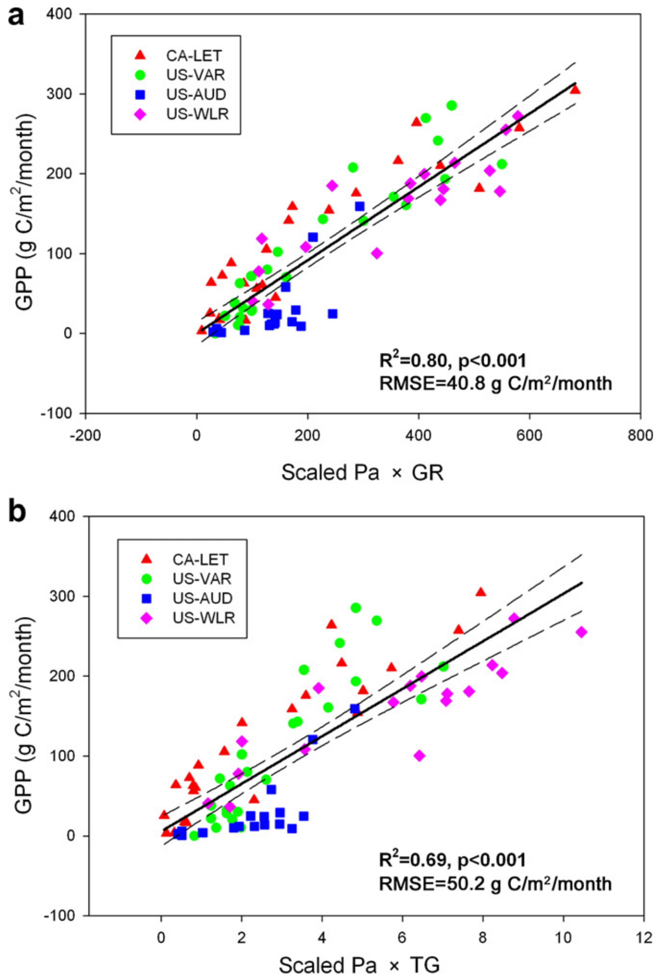

Fig. 6. Estimating monthly GPP using the (a) Scaled$P_a \times$ GR model and (b) Scaled$P_a \times$ TG model.

Precipitation is a variable of high temporal heterogeneity that can vary substantially between months while keep annual quantity relatively stable. The impacts of such variability should be taken into consideration in ecosystem models, especially the changes in precipitation patterns rather than the precipitation quantity (Weltzin et al., 2003). Our results first show a correlation between monthly GPP and precipitation intensity in four grasslands ecosystems. This observation is important and useful as it highlights the importance of precipitation variability obtained from the altered experiments (Knapp et al., 2008; Thomey et al., 2011). Furthermore, this may provide an avenue for the potential use of

Table 4
Comparison between model performances for each site.

Algorithms		GPP models	
		Scaled$P_a \times$ GR	Scaled$P_a \times$ TG
CA-LET	R^2	0.85	0.86
	RMSE	34.3	33.1
US-VAR	R^2	0.87	0.80
	RMSE	31.4	44.0
US-AUD	R^2	0.49	0.50
	RMSE	29.5	28.6
US-WLR	R^2	0.80	0.78
	RMSE	31.7	31.9

Note: RMSE in GPP unit of g C m^{-2} $month^{-1}$.

precipitation patterns in ecological models. With this finding, here we explore the potential use of this precipitation intensity in remote sensing based GPP models in order to improve the accuracy of GPP estimation. This would be useful for the development of future GPP models as it provides a method to link GPP and precipitation patterns at the monthly temporal scale.

4.2. Explanations of better GPP estimates

To better understand the mechanisms of model performances incorporating the P_a scalar, we further explored the responses of both LUE and APAR, two major components in GPP estimation, to the changes in P_a. For the overall dataset, no correlation had been acquired between LUE and P_a (Fig. 7a, $R^2 = 0.00$, $p = 0.472$). However, significant correlation existed for data at CA-LET ($R^2 = 0.28$, $p = 0.012$) and US-AUD ($R^2 = 0.30$, $p = 0.022$), indicating the responses of LUE to P_a may differ for ecosystems at different ecoregions due to its climatic properties. A significant correlation ($p < 0.001$) was acquired between P_a and APAR with coefficient of determination R^2 of 0.49 for the overall dataset, which indicates that future higher precipitation intensity predicted by ecosystem models would help canopies to gain radiation and thus enhancing monthly GPP. These probably are the main reasons for the better performances of the revised models in estimating GPP.

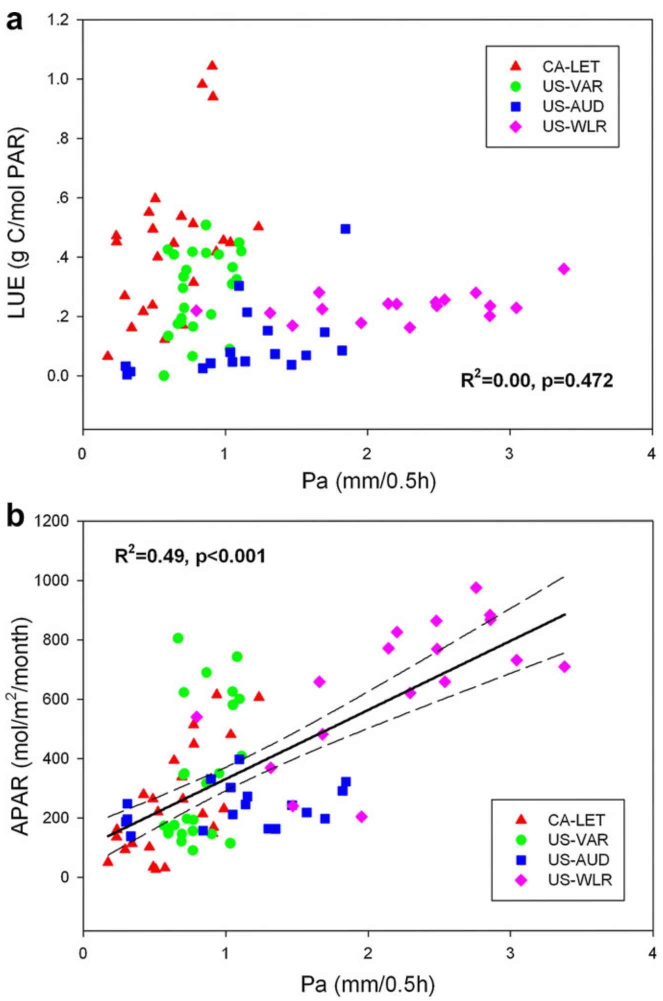

Fig. 7. Relationships between P_a and (a) light use efficiency (LUE) and (b) absorbed photosynthetic active radiation (APAR).

4.3. Potential challenges with precipitation intensity

It is suggested that results in this study would provide the first step in the use of precipitation patterns for future carbon exchange and climate change research. While P_a only shows moderate correlation ($r = 0.39$, $p < 0.001$) with monthly GPP, this relationship is still important as it reveals an additional impact of precipitation patterns on ecological processes, which would probably be overlooked or underestimated. This impact would be useful for the P_a as an ancillary input parameter for future GPP algorithms to better explain the variance in GPP, especially at monthly temporal scale.

Specific attentions are suggested in the further analysis. First, the grasslands are ecosystems that are very sensitive to water availability and can respond to such changes quickly. Although four sites were adopted in this analysis to ensure the relatively wide ranges in precipitation (300–1000 mm/year), there are uncertainties in the application of the revised models in other ecosystems because biomes in mesic environments may have low sensitivity to precipitation changes (Huxman et al., 2004). The feasibility or improvements of revised models may differ for ecosystems in ecoregions facing different water availabilities. This is the possible reason for the different responses of LUE on this precipitation intensity among sites. Second, precipitation is a heterogeneous factor and this will lead to problems in the operational applications. For example, if no precipitation is available in a month, the P_a will not make sense and the production of vegetation can either be very low or even higher, probably dependents on the synchronization between vegetation growing season and precipitation period. The opposite aspect is months with abundant precipitation and the limited times of precipitation which can lead to an extremely large values of P_a. For instance, an overall precipitation of 300 mm is observed in US-VAR with precipitation frequency n of 209 in Dec. 2005. The P_a for this month equals to 1.44 mm/0.5 h, which is three times larger than the standard deviation (sd = 0.17 mm) of all observations after subtracting the P_a average (P_{a}_ave = 0.82 mm) for this site. This “outlier”, excluded in this study from the statistical perspective, would happen in natural ecosystems because precipitation is a stochastic factor that can change dramatically. In these cases, other variables, such as the soil water content and the precipitation of the previous month may be of potential use in those models as the lag effects of the responses of ecosystems to changes in precipitation regimes (Weltzin et al., 2003). The third consideration is the underlying mechanism that links the better performance of GPP models to precipitation intensity. Although we have observed improvements of P_a on the APAR, it is still unclear about the extent of such positive impacts in other ecosystems which indicates that further analyses and validations are particularly desired. The unknown mechanism also prevents a further modification of the temporal resolution of the revised GPP models. The last point limits the use of this precipitation intensity may be the strategy in operational applications. This probably depends both on the sensitivity of vegetation production to precipitation intensity at various temporal scales and the data availability of precipitation frequency at regional to global scales.

5. Conclusion

Future precipitation changes have been demonstrated to have great influences on vegetation production and the precipitation patterns are suggested to play a more important role than the precipitation quantity in these changes (Weltzin et al., 2003). Here we reported an analysis showing that the monthly GPP in four northern grasslands were correlated to the precipitation intensity (P_a) derived from the half-hourly measurements. This precipitation intensity was further normalized to revise two remote sensing based GPP models and results of multi-year analysis indicated that a ScaledP_a can help to improve the monthly GPP estimates by 10% improvement in precision. A possible explanation of such improvements is the positive impacts of P_a on the absorbed radiation. These results provide a possible solution for the incorporation of precipitation intensity in future applications of ecosystem models and validate the role of precipitation patterns in the determination of ecosystem production. The potential use of the revised models in other landscapes is needed and the mechanisms of precipitation intensity on ecosystem production are also the future objectives.

Acknowledgments

We like to provide thanks to Dr. L. B. Flanagan and Dr. D. D. Baldocchi in providing us the flux and ground measurements. This work was funded by an NSERC Strategic Grant (381474-09) and by the National Natural Science Foundation of China (Grant No. 41001210), the Knowledge Innovation Program of CAS (KZCX2-EW-QN302), and the Special Foundation for Young Scientists of IRSA (Y0S04800KB).

References

Barr, A.G., Black, T.A., Hogg, E.H., Kljun, N., Morgenstern, K., Nesic, Z., 2004. Interannual variability in the leaf area index of a boreal aspen-hazelnut forest in relation to net ecosystem production. Agricultural and Forest Meteorology 126, 237–255.

Beer, C., Reichstein, M., Tomelleri, E., Ciais, P., Jung, M., Carvalhais, N., Rödenbeck, C., Arain, M.A., Baldocchi, D., Bonan, G.B., Bondeau, A., Cescatti, A., Lasslop, G., Lindroth, A., Lomas, M., Luyssaert, S., Margolis, H., Oleson, K.W., Roupsard, O., Veenendaal, E., Viovy, N., Williams, C., Ian Woodward, F., Papale, D., 2010. Terrestrial gross carbon dioxide uptake: global distribution and covariation with climate. Science 329, 834–838.

Coops, N.C., Waring, R.H., Law, B.E., 2005. Assessing the past and future distribution and productivity of ponderosa pine in the Pacific Northwest using a process model, 3-PG. Ecological Modelling 183, 107–124.

Easterling, D.R., Meehl, G.A., Parmesan, C., Changnon, S.A., Karl, T.R., Mearns, L.O., 2000. Climate extremes: observations, modeling, and impacts. Science 289, 2068–2074.

Fang, J., Piao, S., Tang, Z., Peng, C., Ji, W., 2001. Interannual variability in net primary production and precipitation. Science 293, 1723.

Flanagan, L.B., Wever, L.A., Carlson, P.J., 2002. Seasonal and interannual variation in carbon dioxide exchange and carbon balance in a northern temperate grassland. Global Change Biology 8, 599–615.

Flanagan, L.B., Johnson, B.G., 2005. Interacting effects of temperature, soil moisture and plant biomass production on ecosystem respiration in a northern temperate grassland. Agricultural and Forest Meteorology 130, 237–253.

Garbulsky, M.F., Penuelas, J., Gamon, J., Inoue, Y., Filella, I., 2011. The photochemical reflectance index (PRI) and the remote sensing of leaf, canopy and ecosystem radiation use efficiencies. Remote Sensing of Environment 115, 281–297.

Gitelson, A.A., Viña, A., Verma, S.B., Rundquist, D.C., Arkebauer, T.J., Keydan, G., Leavitt, B., Ciganda, V., Burba, G.G., Suyker, A.E., 2006. Relationship between gross primary production and chlorophyll content in crops: implications for the synoptic monitoring of vegetation productivity. Journal of Geophysical Research 111, D08S11. doi:10.1029/2005JD006017.

Goetz, S.J., Prince, S.D., Small, J., 2000. Advances in satellite remote sensing of environmental variables for epidemiological applications. Advances in Parasitology 47, 289–307.

Heisler-White, J.L., Knapp, A.K., Kelly, E.F., 2008. Increasing precipitation event size increases aboveground net primary productivity in a semi-arid grassland. Oecologia 158, 129–140.

Hilker, T., Coops, N.C., Wulder, M.A., Black, T.A., Guy, R.D., 2008. The use of remote sensing in light use efficiency based models of gross primary production: a review of current status and future requirements. Science of the Total Environment 404, 411–423.

Huete, A., Didan, K., Miura, T., Rodriguez, E.P., Gao, X., Ferreira, L.G., 2002. Overview of the radiometric and biophysical performance of the MODIS vegetation indices. Remote Sensing of Environment 83, 195–213.

Huxman, T.E., Smith, M.D., Fay, P.A., Knapp, A.K., Shaw, M.R., Loik, M.E., Smith, S.D., Tissue, D.T., Zak, J.C., Weltzin, J.F., Pockman, W.T., Sala, O.E., Haddad, B., Harte, J., Koch, G.W., Schwinning, S., Small, E.A., Williams, D.G., 2004. Convergence across biomes to a common rain-use efficiency. Nature 429, 651–654.

Jastrow, J.D., Miller, R.M., Owensby, C.E., 2000. Long-term effects of elevated atmospheric CO2 on below-ground biomass and transformations to soil organic matter in grassland. Plant and Soil 224, 85–97.

Knapp, A.K., Smith, M.D., 2001. Variation among biomes in temporal dynamics of aboveground primary production. Science 291, 481–484.

Knapp, A.K., Beier, C., Briske, D.D., Classen, A.T., Luo, Y., Reichstein, M., Smith, M.D., Smith, S.D., Bell, J.E., Fay, P.A., Heisler, J.L., Leavitt, S.W., Sherry, R., Smith, B., Weltzin, J., Wend, E., Yarie, J., 2008. Consequences of more extreme precipitation regimes for terrestrial ecosystems. BioScience 58, 811–821.

Krishnan, P., Meyers, T.P., Scott, R.L., Kennedy, L., Heuer, M., 2011. Energy exchange and evapotranspiration over two temperate semi-arid grasslands in North America. Agricultural and Forest Meteorology. doi:10.1016/j.agrformet.2011.09.017.

Mu, Q., Zhao, M., Running, S.W., 2011. Improvements to a MODIS global terrestrial evapotranspiration algorithm. Remote Sensing of Environment 115, 1781–1800.

Norby, R.J., DeLucia, E.H., Gielen, B., Calfapietra, C., Giardina, C.P., King, S.J., Ledford, J., McCarthy, H.R., Moore, D.J.P., Ceulemans, R., De Angelis, P., Finzi, A.C., Karnosky, D.F., Kubiske, M.E., Lukac, M., Pregitzer, K.S., Scarasci-Mugnozza, G.E., Schlesinger, W.H., Oren, R., 2005. Forest response to elevated CO_2 is conserved across a broad range of productivity. Proceedings of the National Academy of Sciences of the United States of America 102, 18052–18056.

Paiva, R.C.D., Buarque, D.C., Clarke, R.T., Collischonn, W., Allasia, D.G., 2011. Reduced precipitation over large water bodies in the Brazilian Amazon shown from TRMM data. Geophysical Research Letters 38, L04406. doi:10.1029/2010GL045277.

Papale, D., Valentini, A., 2003. A new assessment of European forests carbon exchange by eddy fluxes and artificial neural network spatialization. Global Change Biology 9, 525–535.

Reichstein, M., Falge, E., Baldocchi, D., Papale, D., Aubinet, M., Berbigier, P., Bernhofer, C., Buchmann, N., Gilmanov, T., Granier, A., Grunwald, T., Havrankova, K., Ilvesniemi, H., Janous, D., Knohl, A., Laurila, T., Lohila, A., Loustau, D., Matteucci, G., Meyers, T., Miglietta, F., Ourcival, J.M., Pumpanen, J., Rambal, S., Rotenberg, E., Sanz, M., Tenhunen, J., Seufert, G., Vaccari, F., Vesala, T., Yakir, D., Valentini, R., 2005. On the separation of net ecosystem exchange into assimilation and ecosystem respiration: review and improved algorithm. Global Change Biology 11, 1424–1439.

Rouse, J.W., Haas, R.H., Schell, J.A., Deering, D.W., Harlan, J.C., 1974. Monitoring the vernal advancements and retrogradation of natural vegetation. In: NASA/GSFC. Final report, Greenbelt, MD, USA, pp. 1–137.

Ryu, Y., Baldocchi, D.D., Ma, S., Hehn, T., 2008. Interannual variability of evapotranspiration and energy exchange over an annual grassland in California. Journal of Geophysical Research 113, D09104. doi:10.1029/2007JD009263.

Samanta, A., Ganguly, S., Hashimoto, H., Devadiga, S., Vermote, E., Knyazikhin, Y., Nemani, R.R., Myneni, R.B., 2010. Amazon forests did not green-up during the 2005 drought. Geophysical Research Letters 37, L05401. doi:10.1029/2009GL042154.

Sims, D.A., Rahman, A.F., Cordova, V.D., El-Masri, B.Z., Baldocchi, D.D., Bolstad, P.V., Flanagan, L.B., Goldstein, A.H., Hollinger, D.Y., Misson, L., Monson, R.K., Oechel, W.C., Schmid, H.P., Wofsy, S.C., Xu, L., 2008. A new model of gross primary productivity for North American ecosystems based solely on the enhanced vegetation index and land surface temperature from MODIS. Remote Sensing of Environment 112, 1633–1646.

Thomey, M.L., Collins, S.L., Vargas, R., Johnson, J.E., Brown, R.F., Natvig, D.O., Friggens, M.T., 2011. Effect of precipitation variability on net primary production and soil respiration in a Chihuahuan Desert grassland. Global Change Biology 17, 1505–1515.

Weltzin, J.F., Loik, M.E., Schwinning, S., Williams, D.G., Fay, P., Haddad, B., Harte, J., Huxman, T.E., Knapp, A.K., Lin, G., Pockman, W.T., Shaw, M.R., Small, E.E., Smith, M.D., Smith, S.D., Tissue, D.T., Zak, J.C., 2003. Assessing the response of terrestrial ecosystems to potential changes in precipitation. BioScience 53, 941–952.

Wu, C., Munger, J.W., Niu, Z., Kuang, D., 2010. Comparison of multiple models for estimating gross primary production using MODIS and eddy covariance data in Harvard Forest. Remote Sensing of Environment 114, 2925–2939.

Wu, C., Niu, Z., Tang, Q., Huang, W., Rivard, B., Feng, J., 2009. Remote estimation of gross primary production in wheat using chlorophyll-related vegetation indices. Agricultural and Forest Meteorology 149, 1015–1021.

Wu, C., Chen, J.M., Huang, N., 2011. Predicting gross primary production from the enhanced vegetation index and photosynthetically active radiation: evaluation and calibration. Remote Sensing of Environment 115, 3424–3435.

Xiao, X., Hollinger, D., Aber, J., Goltz, M., Davidson, E.A., Zhang, Q., Moore III, Berrien, 2004. Satellite-based modeling of gross primary production in an evergreen needleleaf forest. Remote Sensing of Environment 89, 519–534.

Yang, W., Shabanov, N.V., Huang, D., Wang, W., Dickinson, R.E., Nemani, R.R., Knyazikhin, Y., Myneni, R.B., 2006. Analysis of leaf area index products from combination of MODIS Terra and Aqua data. Remote Sensing of Environment 104, 297–312.

Zhao, M., Running, S.W., 2010. Drought-induced reduction in global terrestrial net primary production from 2000 through 2009. Science 329, 940–943.

Zhao, M., Running, S.W., Nemani, R.R., 2006. Sensitivity of moderate resolution imaging spectroradiometer (MODIS) terrestrial primary production to the accuracy of meteorological reanalyses. Journal of Geophysical Research 111, G01002. doi:10.1029/2004JG000004.